

Giant enhancement of superconductivity in few layers $MoTe_2$

Yuan Gan(甘远), Chang-Woo Cho, Alei Li(李阿蕾), Jian Lyu(吕坚), Xu Du(杜序), Jin-Sheng Wen(温锦生), Li-Yuan Zhang(张立源)

Citation: Chin. Phys. B . 2019, 28(11): 117401 . **doi:** 10.1088/1674-1056/ab457f
Journal homepage: http://cpb.iphy.ac.cn; http://iopscience.iop.org/cpb

What follows is a list of articles you may be interested in

Heat treatment on phase evolution of Bi-2223 precursor powder prepared by spray pyrolysis method

Li-Jun Cui(崔利军), Ping-Xiang Zhang(张平祥), Jin-Shan Li(李金山), Guo Yan(闫果), Yong Feng(冯勇), Xiang-Hong Liu(刘向宏), Jian-Feng Li(李建峰), Xi-Feng Pan(潘熙峰), Fan Yang(杨帆), Sheng-Nan Zhang(张胜楠), Xiao-Bo Ma(马晓波), Guo-Qing Liu(刘国庆)

Chin. Phys. B . 2019, 28(4): 047401 . **doi:** 10.1088/1674-1056/28/4/047401

Synthesis, physical properties, and annealing investigation of new layered Bi-chalcogenide $LaOBiHgS_3$

Yi Yu(于一), Chunchang Wang(汪春昌), Liang Li(李亮), Qiuju Li(李秋菊), Chao Cheng(程超), Shuting Wang(王舒婷), Changjin Zhang(张昌锦)

Chin. Phys. B . 2019, 28(1): 017401 . **doi:** 10.1088/1674-1056/28/1/017401

Electron transport in Dirac and Weyl semimetals

Huichao Wang(王慧超), Jian Wang(王健)

Chin. Phys. B . 2018, 27(10): 107402 . **doi:** 10.1088/1674-1056/27/10/107402

Tunneling field effect transistors based on in-plane and vertical layered phosphorus heterostructures

Shenyan Feng(冯申艳), Qiaoxuan Zhang(张巧璇), Jie Yang(杨洁), Ming Lei(雷鸣), Ruge Quhe(屈贺如歌)

Chin. Phys. B . 2017, 26(9): 097401 . **doi:** 10.1088/1674-1056/26/9/097401

Electronic structure of transition metal dichalcogenides $PdTe_2$ and $Cu_{0.05}PdTe_2$ superconductors obtained by angle-resolved photoemission spectroscopy

Liu Yan, Zhao Jian-Zhou, Yu Li, Lin Cheng-Tian, Hu Cheng, Liu De-Fa, Peng Ying-Ying, Xie Zhuo-Jin, He Jun-Feng, Chen Chao-Yu, Feng Ya, Yi He-Mian, Liu Xu, Zhao Lin, He Shao-Long, Liu Guo-Dong, Dong Xiao-Li, Zhang Jun, Chen Chuang-Tian, Xu Zu-Yan, Weng Hong-Ming, Dai Xi, Fang Zhong, Zhou Xing-Jiang

Chin. Phys. B . 2015, 24(6): 067401 . **doi:** 10.1088/1674-1056/24/6/067401

RAPID COMMUNICATION

Giant enhancement of superconductivity in few layers $MoTe_2$*

Yuan Gan(甘远)[1,2], Chang-Woo Cho[2], Alei Li(李阿蕾)[2], Jian Lyu(吕坚)[2], Xu Du(杜序)[3], Jin-Sheng Wen(温锦生)[1], and Li-Yuan Zhang(张立源)[2,†]

[1] National Laboratory of Solid State Microstructures and Department of Physics, Nanjing University, Nanjing 210093, China
[2] Department of Physics, Southern University of Science and Technology, Shenzhen 518055, China
[3] Department of Physics and Astronomy, Stony Brook University, Stony Brook, NY 11794, USA

(Received 13 May 2019; revised manuscript received 12 September 2019; published online 25 October 2019)

Recently, the layered transition metal dichalcogenide 1T′ $MoTe_2$ has attracted considerable attention due to its non-saturating magnetoresistance, type-II Weyl semimetal properties, superconductivity, and potential candidate for two-dimensional (2D) topological insulator in the single- and few-layer limit. Here in this work, we perform systematic transport measurements on thin flakes of $MoTe_2$ prepared by mechanical exfoliation. We find that $MoTe_2$ flakes are superconducting and have an onset superconducting transition temperature T_c up to 5.3 K, which significantly exceeds that of its bulk counterpart. The in-plane upper critical field ($H_{c2\|}$) is much higher than the Pauli paramagnetic limit, implying that the $MoTe_2$ flakes have Zeeman-protected Ising superconductivity. Furthermore, the T_c and H_{c2} can be tuned by up to 320 mK and 400 mT by applying a gate voltage. Our result indicates that $MoTe_2$ flake is a good candidate for studying exotic superconductivity with nontrivial topological properties.

Keywords: transition metal dichalcogenide, Weyl semimetal, Ising superconductivity, magneto-transport

PACS: 74.25.F–, 74.62.–c, 74.78.–w **DOI:** 10.1088/1674-1056/ab457f

1. Introduction

With the tremendous success of graphene in studying two-dimensional (2D) physics, layered transition metal dichalcogenides (TMDs) have rapidly risen and provided a new platform for investigating new physics and material properties in 2D limit.[1] Unlike graphene, TMDs crystals have a variety of structures with 2H-, 1T-, 1T′-, and T_d-phases.[2] It is well known that most of 2H- and 1T-compounds possess semiconducting behavior, whereas the structure with 1T′ and T_d phases usually exhibits a semimetal structure.[3–6] In addition, TMDs have also been intensively explored for exotic phenomena such as non-saturating magneto-resistance (MR) in WTe_2,[7,8] pressure-induced superconductivity in $MoTe_2$,[9] ionic gated superconductivity in MoS_2,[10] intrinsic Ising superconductivity in $NbSe_2$,[11] *etc*.

Among those TMDs, 1T′ $MoTe_2$ has attracted considerable interest in recent years as a Weyl semimetal candidate.[12–15] Recently, unconventional superconductivity in bulk and few-layer flakes, as well as topological phase transition induced by temperature and strain were reported.[9,16,17] In particular, it was discovered that the superconductivity in $MoTe_2$ flakes is very different from that in the 2H-structure, such as ionic gated MoS_2[10] and thin-layer $NbSe_2$.[11] This is because the 1T′ structure is expected to show anisotropic spin-orbit coupling due to inversion symmetry broken along both in-plane and out-of-plane direction.[17] Moreover, the thin flakes are expected to host the topologically protected edge states, which may be combined with their superconductivity, and thus resulting in nontrivial topological properties. Therefore, thin-flake $MoTe_2$ is a potential candidate for searching topological superconductivity, which has potential applications in quantum computation.[18] As a result, the nature of superconductivity in $MoTe_2$, which remains unclear, needs further studying.

In this article, we investigate the superconducting properties of the mechanically exfoliated few-layer $MoTe_2$ flakes by using transport measurements. As reported in Ref. [19], the surface of $MoTe_2$ is unstable in the ambient condition because of the weak Mo–Te bond energy, which can induce unpredictable surface oxidation and artifacts in film samples. To ensure the intrinsic properties of $MoTe_2$ flakes, we encapsulate $MoTe_2$ by using hexagonal boron nitride (h-BN) film to protect it from oxidizing. As a result, we have successfully fabricated cleaner samples with much fewer defects than the CVD flakes.[17] We find that our $MoTe_2$ flakes are superconducting and have an onset superconducting transition temperature T_c as high as 5.3 K in the thinnest sample (4 nm), measured in this article, which significantly exceeds the reported transition temperature T_c of the bulk counterpart ($\sim$ 0.1 K).[9] Besides, the T_c of the thin flakes can be tuned by as large as 320 mK

*Project supported by the Guangdong Innovative and Entrepreneurial Research Team Program, China (Grant No. 2016ZT06D348), the National Natural Science Foundation of China (Grant No. 11874193), and the Shenzhen Fundamental Subject Research Program, China (Grant Nos. JCYJ20170817110751776 and JCYJ20170307105434022).

†Corresponding author. E-mail: zhangly@sustech.edu.cn

© 2019 Chinese Physical Society and IOP Publishing Ltd

through applying a gate voltage. Hence, our study may provide an attractive material platform for studying new type of superconductivity in the topological environment.

2. Experimental details

Bulk single crystals of 1T′-$MoTe_2$ were synthesized via a flux method with NaCl. The h-BN/$MoTe_2$ heterostructure devices were assembled by using a dry transfer method. First, $MoTe_2$ and h-BN flakes were separately exfoliated onto different SiO_2 (300 nm)/Si substrates by using Scotch tape. Subsequently, we applied a transparent glass slide with polydimethylsiloxane/polypropylene carbonate (PDMS/PPC) films to pick up a large-sized h-BN flake, and then used it to pick up a small $MoTe_2$ flake. Aligned with a micromanipulator stage and through optical microscopy, the chosen $MoTe_2$ flake is transferred to the prefabricated Hall-bar Cr (5 nm)/Au (50 nm) electrodes on an h-BN/SiO_2 (300 nm)/Si substrate. All the mechanic exfoliation and transfer processes were performed in argon gas glove box. Example of an encapsulated h-BN/$MoTe_2$ heterostructure device is shown in Fig. 1(b).

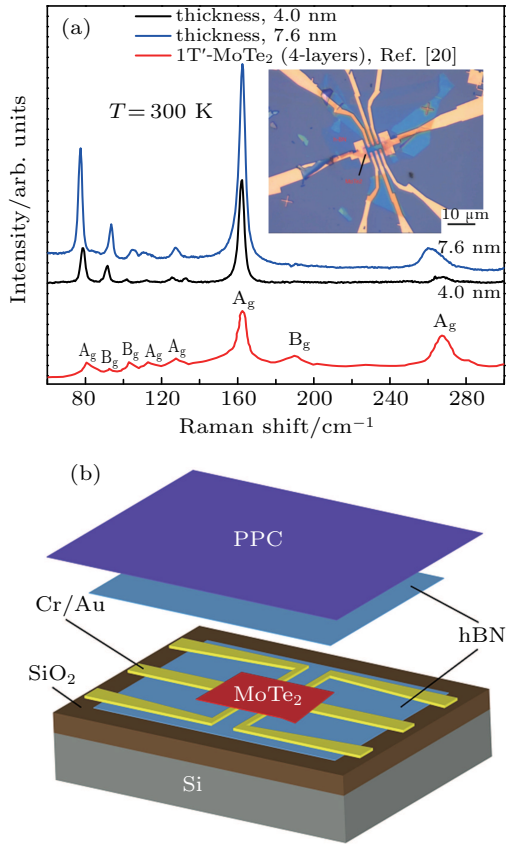


Fig. 1. (a) Measured Raman spectra for 4.0-nm and 7.6-nm $MoTe_2$ sample at 300 K, where red solid curve is for 4-layers $MoTe_2$, which is the same as literature data[30] and inset shows optical microscope image of device $MoTe_2$. (b) Schematics of sandwiched structure of few-layer $MoTe_2$ device.

Raman spectrum was measured with a He–Ne 632.8-nm laser at room temperature. The beam was focused into a diameter of 1 μm, and irradiates the sample through a 25× magnification objective. Magneto-transport measurements are conducted in an Oxford Variable Temperature Insert Measurement System with magnetic field up to 13 T and temperature down to 1.5 K. The resistance is measured by using low-frequency lock-in technique with excitation currents ranging from 0.01 μA to 0.1 μA. The thickness of each sample is determined by the AFM after the transport measurement.

3. Results and discussion

Figure 2(a) shows the normalized resistance ($R/R_{250\,\mathrm{K}}$) as a function of temperature for the exfoliated $MoTe_2$ flakes with thickness ranging from 4.0 nm to 9.3 nm. The sample structure is further characterized by Raman spectra measured at 300 K where we do not find any sign of T_d-phase in thin flakes (*i.e.*, the thickness of 4 nm and 7 nm, see Fig. 1(a)). All samples exhibit a metallic behavior in the whole temperature range before entering into the superconducting state. The well-known first-order structural transition in a $MoTe_2$ single crystal is not observed in our thin-flakes,[17,21] suggesting that thin samples may remain in the 1T′ phase in the low-temperature range.

The residual resistance ratio defined as $RRR = R_{250\,\mathrm{K}}/R_{\mathrm{N}}$, where R_{N} is the normal state resistance above the superconducting transition temperature (here we take N = 10 K), varies from 3.2 (t = 4.0 nm) to 7.5 (t = 9.2 nm), which is approximately twice higher than that of CVD film.[19] From the electrical Hall resistivity extracted through the two-band model (Fig. 2(d)),[22] we can estimate the dominant charge (electron) mobility, μ_{e}, of 4-nm-thick $MoTe_2$ flake at 634 $\mathrm{cm^2/V{\cdot}s}$, *i.e.*, $\mu_{\mathrm{e}} = 634\ \mathrm{cm^2/V{\cdot}s}$, and charge (electron) carrier density n_{e} at $6.4\times10^{18}\ \mathrm{cm^{-3}}$, *i.e.*, $n_{\mathrm{e}} = 6.4\times10^{18}\ \mathrm{cm^{-3}}$. These characteristics compare favorably with what was reported in CVD samples, where $\mu = 40\ \mathrm{cm^2/V{\cdot}s}$ on the 3.8-nm-thick layer which is approximately a factor of 10 lower than our results.[19] In general, the value of RRR and μ both suggest a high-quality sample in the exfoliated $MoTe_2$. Next, we turn to the superconducting properties. A zoom-in of the normalized resistance ($R/R_{10\,\mathrm{K}}$) is shown in the inset of Fig. 2(a) and the layer thickness-dependent critical superconducting transition temperature T_{c} is presented in Fig. 2(b), in which the T_{c} is defined as 90% (black curve) or 60% (red curve) of the normalized $R_{10\,\mathrm{K}}$, respectively. For comparison, we also note the T_{c} of bulk 1T′-$MoTe_2$ crystal used in Ref. [9]. First, all samples show superconductivity below 6 K. However, we do not observe the complete zero resistance due to the base-temperature limitation of our cryostat. An important observation here is that the value of T_{c} significantly rises up to 5.3 K (with criterion of $0.9R_{10\,\mathrm{K}}$) for the 4-nm-thick sample, which is substantially higher than that of bulk $MoTe_2$ ($T_{\mathrm{c}} = 0.1$ K)[9] and $T_{\mathrm{c}} = 3.91$ K of 30-nm-thick T_d-$MoTe_2$.[17]

Generally, as the thickness decreases, disorder and interaction effect will reduce the density of mobile charge carriers, and thus causing its superconductivity to be suppressed and eventually entering into an insulating state in the highly disordered regime,[21,23–25] which is in good agreement with our Hall measurement results as shown in Fig. 2(d). A similar characteristic has been observed in many superconducting materials except for some special cases such as single crystal nanowire arrays.[26,27] Moreover, Cui *et al.* reported the similar thickness dependence of T_c in T_d-$MoTe_2$ very recently.[17,28]

To explain such an enhancement of superconductivity, we try to analyze the electrical Hall resistivity measured at the normal state of 5 K, which are shown in Figs. 2(c) and 2(d). Owing to the fact that the Hall resistivity, ρ_{xy}, exhibits nonlinear magnetic field dependence, we calculate the carrier density and mobility through the two-band model.[22] The dominant carrier (electron) density is nearly constant in a range from 7.6 nm to 4.5 nm and suddenly drops in the thinnest sample (4.0-nm thick). For the case of $MoTe_2$ single crystal, Mandal *et al.* reported an enhancement of T_c after doping it with Re atom, where the maximum T_c reached 4.1 K in $Mo_{0.7}Re_{0.3}Te_2$ composition.[29] They argued that the increase of the electron concentration might contribute to the enhancement of the electron-phonon coupling and density of states at the Fermi energy. However, this is not consistent with our relationship between carrier concentration and T_c.

Another possible scenario is electrochemical doping during the fabrication of thin-flakes: there can appear some doping effects induced by the surface contamination or originating from the silicon oxide substrate. However, we rule out such a scenario based on the comparably higher mobility and *RRR*, which implies that the degradation of our samples is smallest. Moreover, the thin-flakes are weakly coupled to the SiO_2/Si substrate, we believe it is unlikely to be influenced by the oxide substrate.

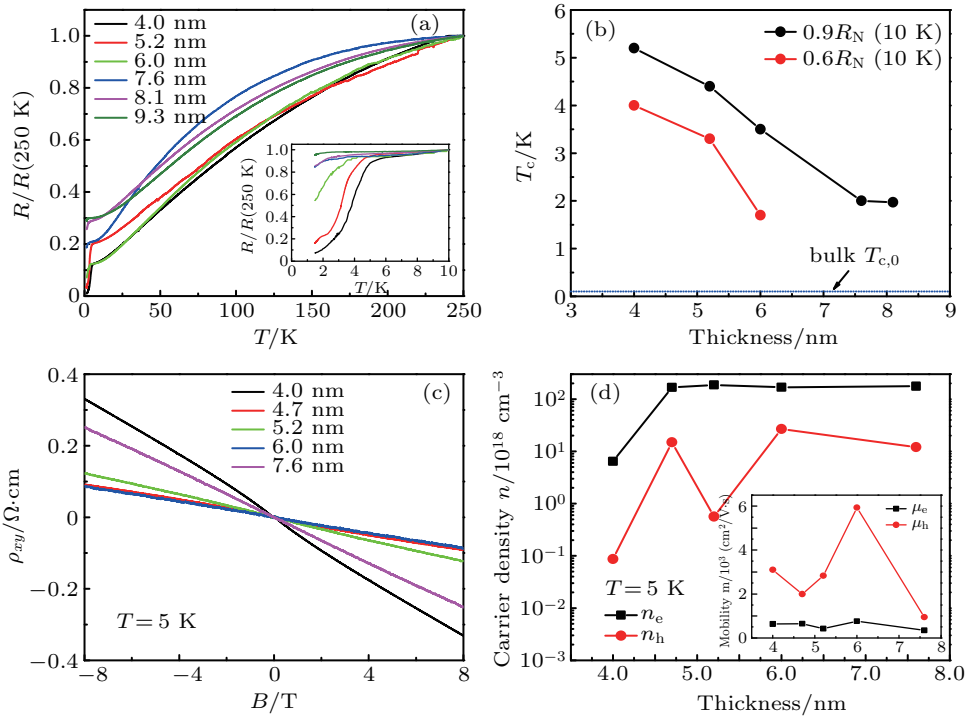


Fig. 2. (a) Temperature dependence of the normalized resistance ($R/R_{250\,K}$) for $MoTe_2$ crystals with thickness ranging from 4.0 nm to 9.3 nm, with inset showing low-temperature zoom-in of the normalized resistance ($R/R_{10\,K}$) as a function of temperature. (b) Superconducting phase transition temperature T_c as a function of sample thickness with T_c being defined as 90% and 60% of normal state resistance at 10 K, and the blue dotted line referring to bulk $T_{c,0}$ cited from Ref. [8]. (c) Electrical Hall resistivity data as a function of a magnetic field for various sample thickness values. (d) Carrier concentration and mobility (inset) at different sample thicknesses at 5 K, extracted from two-band model fit.

Meanwhile, a similar large enhancement of superconductivity was observed in another TMD material TaS_2 in 2016, indicating that the enhancement of the effective electron–phonon coupling plays a crucial role.[30] There it was claimed that the inversed T_c dependence versus the number of layers is due to a relatively strong Coulomb repulsion.[30] Our exfoliated samples are much cleaner with fewer defects than CVD samples. Thus, it may lead the electron-phonon interaction to increase due to a strong screening effect of Coulomb interaction originating from the higher quality samples.[31] Although we discussed several possible scenarios, we are still not clear about the mechanism and origin of T_c enhancement when thickness decreases; these issues remain to be further investigated theoretically and experimentally.

In order to gain a better understanding of the superconductivity properties for exfoliated-flake samples, we map the magnetic field and angular dependence of magneto-resistance (*MR*) and reduced *H*–*T* phase diagram as shown in Fig. 3. Fig-

ures 3(a) and 3(b) clearly show that the dependence of *MR* on magnetic field in a 4-nm-thick $MoTe_2$ crystal at various temperatures (1.5, 2, 3, 5, and 10 K) ((Fig. 3(a)) and field angles, θ (Fig. 3(b)) at a fixed temperature of 1.5 K, where θ denotes the tilt angle between the normal direction of the crystal plane and the magnetic field as depicted in the inset of Fig. 3(c). When the magnetic field is close to the crystal basal plane (θ approaches to 90°), the superconductivity transition shows a higher upper critical field because of its 2D superconductivity nature, which is well matched with 2D Tinkham model fit (Fig. 3(c)). The estimated crystal-plane coherence length $\xi_{\|}$ is ~ 5.5 nm, which is longer than sample thickness. This also supports 2D superconductivity scenario.

In Fig. 3(d), the upper critical field H_{c2} in a parallel field configuration is significantly enhanced due to its strong spin–orbit coupling resulting from inversion symmetry breaking. Although we cannot reach the onset point of H_{c2} at $\theta = 90°$ ($H \|$In-plane) in this study because of the limitation of our superconducting magnet, we still obtain a strikingly strong magnetic anisotropy result ($H_{c2\|}/H_{c2\perp} \sim 22$) in comparison with the magnetic anisotropy of T_d-$MoTe_2$.[17]

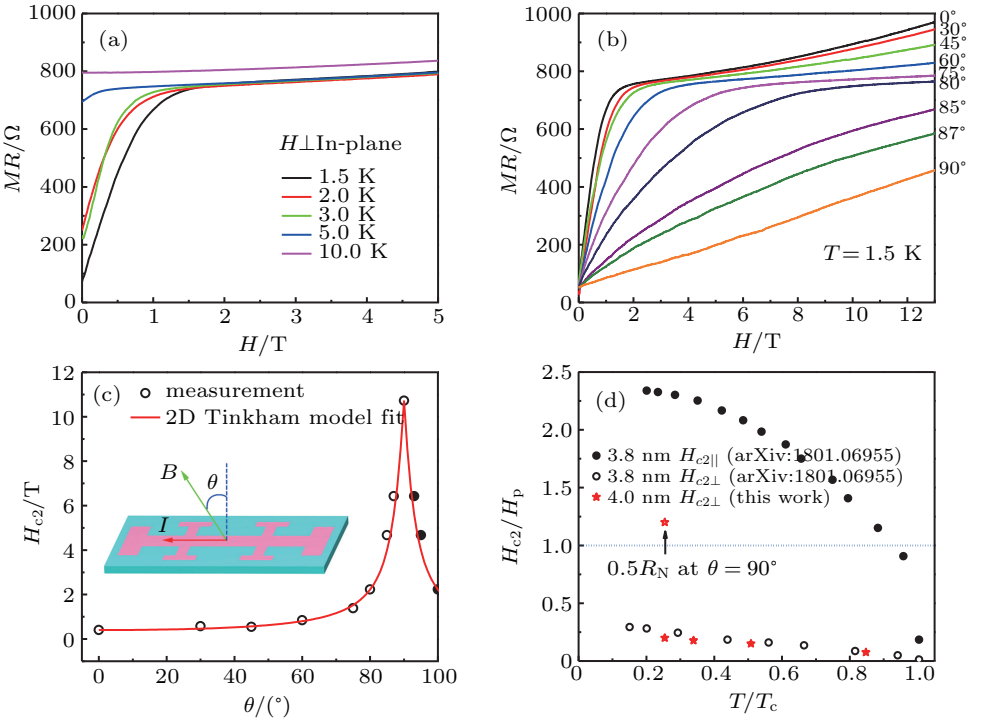


Fig. 3. Plots of magneto-resistance *versus* magnetic field at (a) various temperatures and (b) 1.5 K for different field orientations. All experimental data are taken from 4-nm-thick $MoTe_2$. (c) Angle-dependent upper critical field H_{c2}, with solid red line denoting fitting to the data following the Tinkham formula for a 2D superconductor, and empty circles referring to our data, solid circles representing mirror-symmetrized data for clarity, and inset showing experimental configuration and magnetic field direction. (d) Normalized H–T phase diagram, with symbol red star denoting our data.

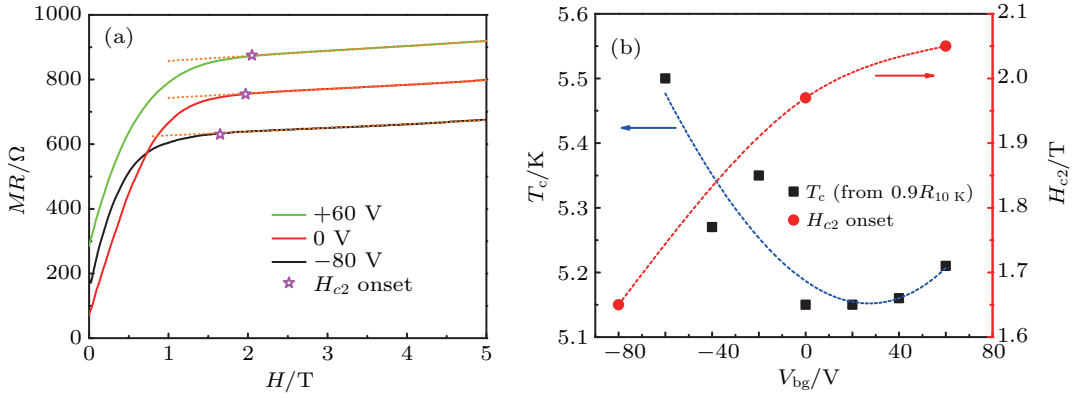


Fig. 4. (a) Variations of magnetoresistance with magnetic fields at 1.5 K for three different back-gate voltages (+60, 0, −80 V). Each dotted line is linear fitting to find onset of corresponding upper critical field. (b) Plot of T_c and H_{c2} *versus* gate voltage, with dotted lines guiding to the eyes.

Finally, we also examine the electric field gating effect with the help of a back-gate sweeping. Figure 4(a) shows that plots of *MR versus* magnetic field for a 4-nm-thick $MoTe_2$ layer with three different gate voltages (+60 V, 0 V, and −80 V). The H_{c2} is determined by a deviation point from the normal state, which is marked with symbol star on the graph.

The applied gate voltage is found to be able to cause T_c and H_{c2} substantially change as shown in Fig. 4(b), with T_c modulation of 320 mK and H_{c2} modulation of 400 mT, corresponding to $\Delta T_c/T_c$ of 6.7% and $\Delta H_{c2}/H_{c2}$ of 16.2%. It is worthy to note that the modulation of T_c and H_{c2} induced by gating effect may be explained from the variation of carrier concentration since other TMD material $NbSe_2$ is reported to have less than 10% modulation by applying gate voltage,[32] which value is more or less consistent with ours. Nevertheless, the large enhancement of T_c as thinned down would be caused by a deeper mechanism, which needs further studying.

4. Conclusions

In this work, we develop a method of fabricating the atomically thin $MoTe_2$ flakes, which minimizes the degradation from exposure to the ambient environment and thus maintains the intrinsic properties of the material. The thin $MoTe_2$ flakes prepared by exfoliation method are characterized to be cleaner with much fewer defects than the CVD-grown samples reported previously. We find that the exfoliated $MoTe_2$ flakes are superconducting and possess an onset superconducting transition temperature T_c of up to 5.3 K, which significantly exceeds the T_c of the bulk counterpart ($\sim$ 0.1 K). The superconductivity in few-layer $MoTe_2$ is consistent with 2D Ising spin crossover as demonstrated by the in-plane magnetoresistance measurement. Moreover, the unconventional superconductivity of the thin film can be modulated by an applied gate voltage, which tunes the T_c and H_{c2} by as large as 320 mK and 400 mT, respectively. These results need further studying in the aspect of TMDs superconductivity in the topology ground.

References

[1] Manzeli S, Ovchinnikov D, Pasquier D, Yazyev O V and Kis A 2017 *Nat. Rev. Mater.* **2** 17033

[2] Revolinsky E and Beerntsen 1966 *J. Phys. Chem. Solids* **27** 523

[3] Splendiani A, Sun L, Zhang Y, Li T, Kim J, Chim C Y, Galli G and Wang F 2010 *Nano Lett.* **10** 1271

[4] Mak K F, Lee C, Hone J, Shan J and Heinz T F 2010 *Phys. Rev. Lett.* **105** 136805

[5] Dawson W and Bullett 1987 *J. Phys. C- Solid State* **20** 6159

[6] Kan M, Nam H G, Lee Y H and Sun Q 2015 *Phys. Chem. Chem. Phys.* **17** 14866

[7] Ali M N, Xiong J, Flynn S, Tao J, Gibson Q D Schoop L M, Liang T, Haldoaarachchige N, Hirschberger M, Ong N P and Cava J 2014 *Nature* **514** 205

[8] Rhodes D, Das S, Zhang Q R, Zeng B, Pradhan N R, Kikugawa N, Manousakis E and Balicas L 2015 *Phys. Rev. B* **92** 125152

[9] Qi Y, Naumov P G, Ali M N, Rajamathi C R, Schnelle W, Barkalov O, Hanfl, M, Wu S C, Shekhar C, Sun Y, Süß V, Schmidt M, Schwarz U, Pippel E and Medvedev S A 2016 *Nat. Commun.* **7** 11038

[10] Lu J M, Zheliuk O, Leermakers I, Yuan N F Q, Zeitler U, Law K T and Ye J T 2015 *Science* **350** 1353

[11] Xi X, Wang Z, Zhao W, Park J H, Law K T, Berger H, Forró L, Shan J and Mak K F 2016 *Nat. Phys.* **12** 139

[12] Chen C, Peng H, Hwang C C, Sun S Z, Mo S K, Vobornik I, Fujii J, Parkin S S P, Felser C, Yan B H and Chen Y L 2017 *Nat. Commun.* **8** 13973

[13] Chang T R, Xu S, Chang G, Lee C, Huang S, Wang B, Bian G, Zheng H, Sanchez D S, Belopolski I, Alidoust N, Neupane M, Bansil A, Jeng H, Lin H and Zahid Hasan M 2016 *Nat. Commun.* **7** 10639

[14] Tamai A, Wu Q S, Cucchi I, Bruno F Y, Riccò S, Kim T K, Hoesch M, Barreteau C, Giannini E, Besnard C, Soluyanov A A and Baumberger F 2016 *Phys. Rev. X* **6** 031021

[15] Wang Z, Gresch D, Soluyanov A A, Xie W, Kushwaha S, Dai X, Troyer M, Cava R J and Bernevig B A 2016 *Phys. Rev. Lett.* **117** 56805

[16] Chen F C, Luo X, Xiao R C, Lu W J, Zhang B, Yang H X, Li J Q, Pei Q L, Shao D F, Zhang R R, Ling L S, Xi C Y, Song W H and Sun Y P 2016 *Appl. Phys. Lett.* **108** 162601

[17] Cui J, Li P, Zhou J, He W Y, Huang X, Yi J, Fan J, Ji Z, Jing X, Qu F, Cheng Z G, Yang C, Lu L, Suenaga K, Liu J, Law K T, Lin J, Liu Z and Liu G 2019 *Nat. Commun.* **10** 2044

[18] Fu L and Kane C L 2008 *Phys. Rev. Lett.* **100** 96407

[19] Yang L, Wu H, Zhang W, Chen Z, Li J, Lou X, Xie Z, Zhu R and Chang H 2018 *Nanoscale* **10** 19906

[20] Beams R, Cancado L G, Krylyuk S, Kalish I, Kalanyan B, Singh A K, Choudhary K, Bruma A, Vora P M, Tavazza F, Davydov A V and Stranick S J 2016 *ACS Nano* **10** 9626

[21] Song P, Hsu C, Zhao M, Zhao X, Chang T R, Teng J, Lin H and Loh K P 2018 *2D Mater.* **5** 31010

[22] Zhou Q, Rhodes D, Zhang Q R, Tang S, Schonemann R and Balicas L 2016 *Phys. Rev. B* **94** 121101(R)

[23] Hebard A F and Vandenberg J M 1980 *Phys. Rev. Lett.* **44** 50

[24] Yazdani A and Kapitulnik A 1995 *Phys. Rev. Lett.* **74** 3037

[25] Okuma S, Terashima T and Kokubo N 1998 *Phys. Rev. B* **58** 2816

[26] Zhang Y, Wong C H, Shen J, Sze S T, Zhang B, Zhang H, Dong Y, Xu H, Yan Z, Li Y, Hu X and Lortz R 2016 *Sci. Rep.* **6** 32963

[27] He M, Wong C H, Tse P L, Zheng Y, Zhang H, Lam F L Y, Sheng P, Hu X and Lortz R 2013 *ACS Nano* **7** 4187

[28] He R, Zhong S, Kim Hyun H, Ye G, Winford L, McHaffie R I, Chen F, Luo X, Sun Y and Tsen W A 2018 *Phys. Rev. B* **97** 041410(R)

[29] Mandal M, Marik S, Sajilesh K P, Arushi, Singh D, Chakraborty J, Ganguli N and Singh R P 2018 *Phys. Rev. Mater.* **2** 094201

[30] Navarro-Moratalla E, Isl, J O, Mañas-Valero S, Pinilla-Cienfuegos E, Castellanos-Gomez A, Quereda J, Rubio-Bollinger G, Chirolli L, Silva-Guillén J A, Agraït N, Steele G A, Guinea F, van der Zant H S J and Coronado E 2016 *Nat. Commun.* **7** 11043

[31] Takahashi H, Akiba T, Imura K, Shiino T, Deguchi K, Sato N K, Sakai H, Bahramy M S and Ishiwata S 2017 *Phys. Rev. B* **95** 100501

[32] Xi X, Berger H, Forró L, Shan J and Mak K F 2016 *Phys. Rev. Lett.* **117** 106801